

SANDER MIRME

Development of nanometer
aerosol measurement technology



TARTU UNIVERSITY PRESS

The study was carried out at the Institute of Physics, University of Tartu, Estonia.

The Dissertation was admitted on June 17, 2011, in partial fulfilment of the requirements for the degree of Doctor of Philosophy in physics (environmental physics), and allowed for defence by the Council of the Institute of Physics, University of Tartu.

Supervisor: Aadu Mirme, Ph.D.
Senior research associate
Institute of Physics
University of Tartu

Opponents: Professor Jorma Keskinen, Ph.D.
Department of Physics
Tampere University of Technology

Kalju Eerme, Ph.D.
Senior research associate
Department of Atmospheric Physics
Tartu Observatory

Defence: August 22, 2011, University of Tartu, Estonia

ISSN 1406-0310
ISBN 978-9949-19-738-5 (trükis)
ISBN 978-9949-19-739-2 (PDF)

Autoriõigus Sander Mirme, 2011

Tartu Ülikooli Kirjastus
www.tyk.ee
Tellimuse nr. 440

Abstract

Formation of aerosol by the nucleation of particles and their subsequent growth has been observed in the atmosphere almost everywhere around the world. The formed particles, initially of nanometer size, may grow further, participate in cloud formation, influence the radiation balance and ultimately climate. On local scales, these particles can affect atmospheric visibility and human health.

There is a growing interest in studying new particle formation. However, it is difficult to measure aerosol particles in the size range of a few nanometers under atmospheric conditions.

An instrument that is well suited for such measurements is the Nanometer aerosol and Air Ion Spectrometer (NAIS, developed by Airel Ltd., Estonia) which uses the principle of electrical aerosol spectrometry to measure the size distributions of naturally charged particles (ions) of both polarities as well as uncharged particles. The NAIS has been specifically designed for atmospheric nanometer aerosol monitoring. It can operate for long periods in a wide range of ambient conditions from polluted downtown to remote forest. It is based on the Air Ion Spectrometer (AIS).

The NAIS uses unipolar corona charging and parallel electrical mobility analysis. The instrument contains two identical multichannel electrical mobility analyzer columns: one for positive, one for negative ions. The aerosol is synchronously mobility-classified in the mobility analyzers and measured with an array of 21 electrometers per column. The NAIS measures the distribution of ions (charged particles and cluster ions) in the electric mobility range from 3.2 to $0.0013 \text{ cm}^2 \text{ V}^{-1} \text{ s}^{-1}$ and the distribution of aerosol particles in the size range from 2.0 to 40 nm. There are more than ten NAIS instruments in use today around the world.

The thesis focuses on the development of the NAIS. The mathematical and technical principles of the instrument are presented. An updated version of the instrument is introduced – the so called “Airborne NAIS”, which is capable of operating on board an aircraft at varying altitudes. The better reliability, adaptability and measurement speed improve regular ground based measurements as well.

Contents

Abstract	5
Nomenclature	8
List of publications	10
1 Introduction	13
1.1 Nanometer range aerosol measurement methods	13
1.2 Electrical aerosol measurement	14
1.3 Theses	15
2 Mathematical principles of parallel electrical aerosol spectrometry	16
2.1 Particle charging	16
2.2 Mobility analysis	17
2.3 Relationship between particle size and electrical mobility . . .	18
2.4 Mathematical model	19
2.5 Spectrum model	19
2.5.1 Evaluation of the spectrum	20
2.5.2 Regularization of the inversion	21
2.5.3 Correction of negative concentration values	22
3 Design of the Nanometer aerosol and Air Ion Spectrometer	23
3.1 General principle	23
3.2 Sample preconditioning	24
3.2.1 Chargers	25
3.3 Mobility analysis	27
3.3.1 Post-filter adjustment	29
3.3.2 Airflows	29
3.4 Electric current measurement	30
3.4.1 Offset correction	30
3.4.2 Outlier removal	31
3.4.3 Filtering	32
3.4.4 Electrometer resets	32
4 Results	34
4.1 Measurement campaigns	34
4.2 Airborne measurements	35
4.3 Instrument verification	39

5	Review of papers and author's contributions	40
6	Conclusions	41
	Bibliography	42
	Acknowledgements	48
	Summary in Estonian	49
	Publications	51

Nomenclature

α	Charging parameter
η	Viscosity of air
λ	Regularization vector
Φ	Flow rate
ϕ	Spectrum vector
$\phi^j(r)$	Elementary particle distribution function j
Φ_a	Sample aerosol flow rate
ϕ_j	Concentration of elementary distribution j
Φ_s	Sheath air flow rate
σ	Electrical conductivity of air
ε_0	Permittivity of vacuum
C	Electrical capacitance
D	Covariance matrix of the section currents
e	Elementary charge $1.6 \cdot 10^{-19}$ C
$f(r)$	Distribution function
$G(i, z)$	Mobility analyzer section i response for ions with mobility z
H	Apparatus matrix
I_i	Electrical current to the analyzer section i
k	Universal gas constant
l	Particle mean free path
n	Particle concentration
P	Air pressure
$P(q, r)$	Probability that a particle with the radius r carries q elementary charges
r	Particle radius
T	Temperature
U	Electric potential, electric voltage
V	Information matrix of the particle spectrum
W	Covariance matrix of the particle spectrum

y	Instrument record vector consisting of section currents I_i
z	Electrical mobility of a particle
z_i	Electrical mobility of charger ions

List of publications

The thesis is based on the following publications:

- I. **S. Mirme**, A. Mirme, A. Minikin, A. Petzold, U. Hörrak, V.-M. Kerminen, and M. Kulmala. Atmospheric sub-3 nm particles at high altitudes. *Atmos. Chem. Phys.*, 10(2):437–451, 2010.
- II. H. E. Manninen, T. Nieminen, E. Asmi, S. Gagné, S. Häkkinen, K. Lehtipalo, P. Aalto, M. Vana, A. Mirme, **S. Mirme**, U. Hörrak, C. Plass-Dülmer, G. Stange, G. Kiss, A. Hoffer, N. Törő, M. Moerman, B. Henzing, G. de Leeuw, M. Brinkenberg, G. N. Kouvarakis, A. Bougiatioti, N. Mihalopoulos, C. O’Dowd, D. Ceburnis, A. Arneth, B. Svenningsson, E. Swietlicki, L. Tarozzi, S. Decesari, M. C. Facchini, W. Birmili, A. Sonntag, A. Wiedensohler, J. Boulon, K. Sellegri, P. Laj, M. Gysel, N. Bukowiecki, E. Weingartner, G. Wehrle, A. Laaksonen, A. Hamed, J. Joutsensaari, T. Petäjä, V.-M. Kerminen, and M. Kulmala. EUCAARI ion spectrometer measurements at 12 European sites – analysis of new particle formation events. *Atmos. Chem. Phys.*, 10(16):7907–7927, 2010.
- III. A. Mirme, E. Tamm, G. Mordas, M. Vana, J. Uin, **S. Mirme**, T. Bernotas, L. Laakso, A. Hirsikko, and M. Kulmala. A wide range multi-channel air ion spectrometer. *Boreal Env. Res.*, 12:247–264, 2007.

Other related publications of the dissertant:

1. T. Suni, M. Kulmala, A. Hirsikko, T. Bergman, L. Laakso, P. P. Aalto, R. Leuning, H. Cleugh, S. Zegelin, D. Hughes, E. van Gorsel, M. Kitchen, M. Vana, U. Hörrak, **S. Mirme**, A. Mirme, S. Sevanto, J. Twining, and C. Tadros. Formation and characteristics of ions and charged aerosol particles in a native Australian eucalypt forest. *Atmos. Chem. Phys.*, 8(1):129–139, 2008.
2. E. Asmi, M. Sipilä, H. E. Manninen, J. Vanhanen, K. Lehtipalo, S. Gagné, K. Neitola, A. Mirme, **S. Mirme**, E. Tamm, J. Uin, K. Komasaare, M. Attoui, and M. Kulmala. Results of the first air ion spectrometer calibration and intercomparison workshop. *Atmos. Chem. Phys.*, 9(1):141–154, 2009.
3. H.E. Manninen, T. Petäjä, E. Asmi, I. Riipinen, T. Nieminen, J. Mikkilä, U. Hörrak, A. Mirme, **S. Mirme**, L. Laakso, et al. Long-term field measurements of charged and neutral clusters using neutral

- cluster and air ion spectrometer (nais). *Boreal Env. Res*, 14:591–605, 2009.
4. M. Kulmala, I. Riipinen, T. Nieminen, M. Hulkkonen, L. Sogacheva, H. E. Manninen, P. Paasonen, T. Petäjä, M. Dal Maso, P. P. Aalto, A. Viljanen, I. Usoskin, R. Vainio, **S. Mirme**, A. Mirme, A. Minikin, A. Petzold, U. Hörrak, C. Plaß-Dülmer, W. Birmili, and V.-M. Kerminen. Atmospheric data over a solar cycle: no connection between galactic cosmic rays and new particle formation. *Atmos. Chem. Phys.*, 10(4):1885–1898, 2010.
 5. V.-M. Kerminen, T. Petäjä, H. E. Manninen, P. Paasonen, T. Nieminen, M. Sipilä, H. Junninen, M. Ehn, S. Gagné, L. Laakso, I. Riipinen, H. Vehkamäki, T. Kurten, I. K. Ortega, M. Dal Maso, D. Brus, A. Hyvärinen, H. Lihavainen, J. Leppä, K. E. J. Lehtinen, A. Mirme, **S. Mirme**, U. Hörrak, T. Berndt, F. Stratmann, W. Birmili, A. Wiedensohler, A. Metzger, J. Dommen, U. Baltensperger, A. Kiendler-Scharr, T. F. Mentel, J. Wildt, P. M. Winkler, P. E. Wagner, A. Petzold, A. Minikin, C. Plass-Dülmer, U. Pöschl, A. Laaksonen, and M. Kulmala. Atmospheric nucleation: highlights of the EUCAARI project and future directions. *Atmos. Chem. Phys.*, 10(22):10829–10848, 2010.
 6. M. Ehn, H. Junninen, S. Schobesberger, H.E. Manninen, A. Franchin, M. Sipilä, T. Petäjä, V.M. Kerminen, H. Tammet, A. Mirme, **S. Mirme**, et al. An instrumental comparison of mobility and mass measurements of atmospheric small ions. *Aerosol Science and Technology*, 45(4):522–532, 2011.
 7. A. Hirsikko, T. Nieminen, S. Gagné, K. Lehtipalo, H. E. Manninen, M. Ehn, U. Hörrak, V.-M. Kerminen, L. Laakso, P. H. McMurry, A. Mirme, **S. Mirme**, T. Petäjä, H. Tammet, V. Vakkari, M. Vana, and M. Kulmala. Atmospheric ions and nucleation: a review of observations. *Atmos. Chem. Phys.*, 11(2):767–798, 2011.
 8. S. Gagné, K. Lehtipalo, H. E. Manninen, T. Nieminen, S. Schobesberger, A. Franchin, T. Yli-Juuti, J. Boulon, A. Sonntag, **S. Mirme**, A. Mirme, U. Hörrak, T. Petäjä, E. Asmi, and M. Kulmala. Intercomparison of air ion spectrometers: an evaluation of results in varying conditions. *Atmospheric Measurement Techniques*, 4(5):805–822, 2011.

9. H. E. Manninen, A. Franchin, S. Schobesberger, A. Hirsikko, J. Hakala, A. Skromulis, J. Kangasluoma, M. Ehn, H. Junninen, A. Mirme, **S. Mirme**, M. Sipilä, T. Petäjä, D. R. Worsnop, and M. Kulmala. Characterisation of corona-generated ions used in a Neutral cluster and Air Ion Spectrometer (NAIS). *Atmospheric Measurement Techniques Discussions*, 4(2):2099–2125, 2011.

1 Introduction

The atmosphere of Earth is an aerosol, i.e. a mixture of gases and solid or liquid particles suspended in it (Fuchs, 1964). Atmospheric aerosol particles directly affect our climate and health.

Atmospheric aerosol is in constant change – existing particles disappear by evaporation, coagulation, precipitation and new particles are formed or introduced.

Depending on their origin, atmospheric aerosol particles are classified as primary or secondary. Primary aerosol particles are produced directly from the solid or liquid phase: e.g. dust, pollen, dispersed water blown up by the wind or residue from combustion. A secondary aerosol particle is formed by processes taking place in the gaseous phase resulting the formation of a tiny droplet, i.e. nucleation.

Initially the nucleated particles are very small, about 1 nm in diameter. Subsequently they may grow by condensing vapors and coagulating with other particles. They will participate in cloud formation, influence the radiation balance and ultimately climate. On local scales, the particles may influence atmospheric visibility and human health. Formation of aerosol particles by nucleation and their growth has been observed in the atmosphere almost everywhere around the world (Kulmala et al., 2004). Yet its magnitude and driving factors are still poorly understood (Kulmala et al., 2007b).

1.1 Nanometer range aerosol measurement methods

Aerosol is difficult to measure. The shape, size and chemical composition of particles varies widely. Particles are detected either by their mass by collecting them on a filter, optically by detecting scattered light pulses or electrically by measuring particle electric charge flux or electric current from electrically charged particles depositing on an electrode.

It is especially difficult to measure the smallest particles in the size range of a few nanometers under atmospheric conditions. A number of aerosol instruments can sense fine nanometer range particles and measure their concentration in the atmosphere using the principle of condensational growth and optical counting (CPC, McMurry, 2000). Information about particle size variations is practically lost. However, for understanding atmospheric aerosol processes, it is necessary to know the particle size distribution.

Some information about particle size can be acquired by combining the readings of several particle counters with different cut-off sizes (Kulmala et al., 2007a) or by analyzing the pulse height of the instrument response

(Marti et al., 1996). The methods exhibit some dependence on particle chemical composition.

Nanometer range particles are not directly optically detectable. Thus methods simply relying on particle light scattering are not suitable. Inertial methods work fine for large particles but not in nanometer range.

1.2 Electrical aerosol measurement

The particle distribution in a broad particle size range can be measured by spectrometers that use electrical mobility classification.

Some instruments (e.g. SMPS or DMPS; Wang & Flagan, 1990) use aerosol neutralizers to give the particles a determined electric charge distribution, and then scan over a range on particle electrical mobilities using a differential mobility analyzer (DMA). The DMA output is measured using a condensation particle counter (CPC). Due to the limitations of the CPC, the smallest mobility equivalent particle size that can be measured by these instruments is typically 3 nm.

Distributions of particles with sizes below 3 nm can be measured by some instruments that sense air ions, i.e. particles with an electric charge: e.g. AIS (Mirme et al., 2007), BSMA (Tammet, 2006), SIGMA (Tammet, 2011). As these instruments do not sense uncharged particles, a big fraction of aerosol is left unmeasured.

An electrical aerosol instrument assesses the concentration of particles based on a known probability distribution of electric charge on particles that have been charged in well-defined conditions. The obtained charge is strongly dependent on particle size. After charging, the particles are mobility classified and detected by their carried electric charge. So the principal elements of the method are particle charging, mobility analysis, charge collection/detection and finally spectrum deconvolution.

Towards smaller particles, the charging probability decreases and particle loss increases which causes the electric response signal to drop gradually. Thus the lowest detectable size limit is determined by the efficiency of the charger and the sensitivity of the charge collection.

The electrical method has good potential to be used for measuring nanometer range aerosol:

- The sampled particles are only treated electrically by processes which are naturally occurring in the atmosphere as well.
- The method virtually does not have a dependency on the chemical composition of the particles.

- There is no principal size limit for measuring naturally charged ions, for uncharged particles the size limit is determined by the size of charger ions.

1.3 Theses

The focus of the thesis is the development of an electrical aerosol instrument capable of measuring nanometer aerosol in fast varying atmospheric conditions – the Nanometer aerosol and Air Ion Spectrometer (NAIS). The mathematical and technical principles of the instrument are presented. An upgraded version of the NAIS is introduced. Most of the work has been done to make the instrument more reliable and adaptable to different environments and to improve its sensitivity and time resolution.

The main theses are:

1. The NAIS is capable of measuring alternately nanometer aerosol and cluster-ions.
2. The NAIS is a suitable instrument for long term atmospheric monitoring and it can be used to detect nucleation events everywhere around the world.
3. With some enhancements, The NAIS technology is capable of measuring under difficult conditions like low atmospheric pressure, rapidly varying aerosol.
4. The NAIS can measure nanometer aerosol throughout the tropospheric column on board an aircraft.

2 Mathematical principles of parallel electrical aerosol spectrometry

A parallel electrical aerosol spectrometer is essentially a DMA with many output sections and measurement channels. Instead of varying the analyzer voltage to scan over a range of particle mobilities, the whole distribution is captured at once (Israel, 1931; Yunker, 1940).

All the sampled particles are collected on measurement electrodes all of the time, so no signal is lost. This provides higher measurement sensitivity but also makes the measurement result more reliable in case quickly changing aerosol distributions which may produce false spectra for scanning instruments.

To allow the instrument to measure uncharged particles, the sample is passed through a charger before the mobility analyzer. The best charging efficiency is achieved using unipolar charging. The easiest way to produce a unipolar charger ion field is corona discharge.

Instruments based on the method of parallel electrical aerosol spectrometry have been developed at the University of Tartu since 1970's (Jakobson et al., 1975; Mirme et al., 1984).

2.1 Particle charging

In the corona charger, the particles pass through a cloud of charger ions of a single polarity. In order to calculate the particle size distribution from the collected charge in the mobility analyzer, it is necessary to know the charge distribution of particles exiting the charger.

The probability of a particle acquiring electric charge at a given moment depends on the particle diameter, already present charge on the particle, global electric field strength and charger ion density. The process is viewed as a flux of ions onto the particle which is calculated using the kinetic theory (Podolsky, 1977) inside the limiting sphere around a particle (Fuchs, 1963). The radius of the limiting sphere is a parameter determined during the calibration of the instrument.

The change of the charge probability distribution is calculated by integrating a birth-death differential equation (Boisdron & Brock, 1970) along the particle trajectory through the charger. An integral formula (Salm, 1992) is used to produce the complete distribution. The formula allows to calculate the final charge distribution for an arbitrary initial charge distribution, e.g. for the case that the particles are initially in a bipolar equilibrium charging state.

The charger is characterized with the charging parameter α (Tammet, 1992):

$$\alpha = \frac{1}{\varepsilon_0} \int \sigma dt , \quad (1)$$

where ε_0 is the permittivity of vacuum and $\sigma = ez_i n$ is the electrical conductivity of air (e is the elementary charge, z_i is the electrical mobility of charging ions, and n the ion concentration). The exact value of the charging parameter is determined at the calibration.

2.2 Mobility analysis

The mobility analyzer of a parallel electrical aerosol instrument consists of a number of cylindrical electrodes (Figure 1). The central electrode is divided into several sections as well, each biased at a different fixed electric potential to extend the mobility range while limiting the size of the instrument.

The charge collecting outer electrodes are connected to electrometric amplifiers at near ground potential which in turn are connected to a data acquisition system.

The charged aerosol is sucked into an circular opening near the central electrode. The clean sheath air is introduced near the outer electrode. The particles travel along the analyzer and those with the same charge electrical polarity as the central electrode are pushed towards the outer electrodes by a radial electric field. The particles that have been deposited on a collecting section pass their charge on to the respective amplifier.

The electric mobility analysis follows the generic aspiration theory (Tammet, 1970). According the theory, the movement of a charged particle in a cylindrically symmetrical analyzer is determined by the air flow rate (Φ) and the electric field ($C \cdot U$ product, where C is the analyzer capacitance, U is the analyzer voltage) that is crossed by the particle while traveling inside the analyzer.

$$z = \frac{\Phi \cdot \varepsilon_0}{C \cdot U} \quad (2)$$

The formula determines the relationship between three parameters: flow rate Φ , particle mobility z and analyzer capacitance C . Fixing one of them fixes the ratio of the other two. So an ion with the mobility z attaching to an outer electrode has passed the flow rate Φ and the electric field $C \cdot U$. This allows to calculate the attachment locations of ions with different mobilities

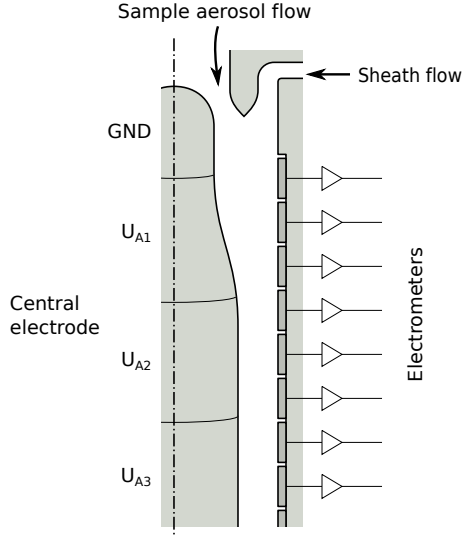


Figure 1: Schematic of NAIS mobility analyzer

entering the analyzer at different flow rates. The formula can be modified for the analyzer, consisting of multiple sections as follows:

$$z_n = \frac{(\Phi_a + \Phi_s) \cdot \varepsilon_0}{\sum_{i=0}^n C_i \cdot U_i}, \quad (3)$$

where Φ_a is the sample aerosol flow rate and Φ_s is the sheath flow rate, z_n is the lowest (limiting) mobility of particles reaching the the section n .

2.3 Relationship between particle size and electrical mobility

To relate the particle mobility measured by the mobility analyzer to particle size and electric charge the conversion by Millikan (Fuchs, 1964) is commonly used.

$$z_{\text{Millikan}} = e \frac{1 + \frac{l}{r} [a + b \exp(-c \frac{r}{l})]}{6\pi\eta r} \quad (4)$$

where a , b and c are empirical constants, e is the elementary charge, l is the particle mean free path and η is the viscosity of air. The mobility of a particle of a given size is a function of ambient atmospheric pressure and temperature.

For small particles a correction has been proposed by Tammet (Tammet, 1995).

2.4 Mathematical model

The instrument response of the parallel electrical aerosol spectrometer is proportional to particle concentration, i.e. the mathematical model of the measurement process is linear. The rule is only broken in the case of very high concentrations when there is no longer an abundance of charger ions to charge all particles.

The instrument response is a set of electric currents that are generated by the flux of ions precipitating to the analyzer sections. Each section current I_i equals the sum of the charge flux of all aerosol particles of the size distribution $f(r)$ that reach the section i :

$$I_i = \int \left[e \sum_q q G(i, z) P(q, r) \right] f(r) dr, \quad (i = 1, \dots, n), \quad (5)$$

where $G(i, z)$ is the response of analyzer section i to ions with mobility $z = z(q, r)$, $P(q, r)$ is the probability that a particle with radius r carries q elementary charges (e).

In the case of an ion analyzer, where the charger is not used and only naturally charged particles are considered (electric charge $q = 1$ and charging probability function $P = 1$), the response function G is equal to the amount of airflow from which the ions of the given mobility are attached to the given analyzer section.

The system of equations (5) links the unknown aerosol distribution $f(r)$ with the measured currents I_i ($i = 1, \dots, n$). The equations should fully consider the instrument specificity (charging, mobility analysis, etc.).

2.5 Spectrum model

The task of spectrometry is to solve instrument response equation (5) i.e. to find the aerosol distribution $f(r)$ from the measured channel currents.

The task is mathematically incorrect. An approximate solution is possible the information required for the description of the aerosol distribution is limited. Therefore the aerosol distribution is estimated as a sum of m elementary distributions of predefined shapes $\phi^j(r)$ (7) (Figure 2).

$$f(r) = \sum_j \phi_j \cdot \phi^j(r), \quad (j = 1, \dots, m) \quad (6)$$

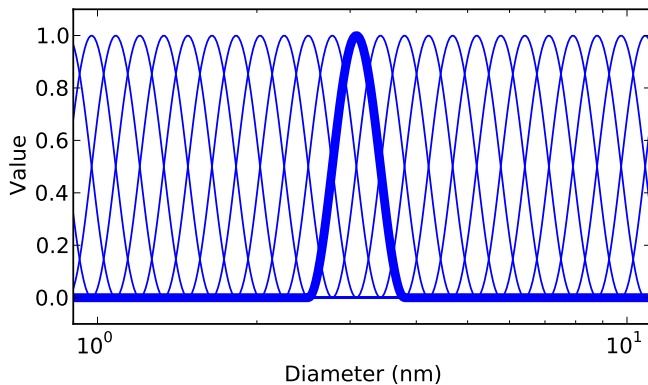


Figure 2: Part of a typical set of elementary distributions with one distribution highlighted.

The set is chosen based on the capabilities of the instrument and the data inversion. This way an aerosol distribution is described by a set of coefficients ϕ_j (a spectrum) and the integral instrument response equations (5) can be transformed into a set of linear equations (7) or the equivalent matrix form (8).

$$I_i = \sum_j H_{ij} \cdot \phi_j, \quad (i = 1, \dots, n) \quad (7)$$

$$y = H \cdot \phi \quad (8)$$

The instrument record vector y consists of section currents I_i and the spectrum vector ϕ consists of coefficients ϕ_j . Matrix H can be called an apparatus matrix. The matrix element H_{ij} is the response of the analyzer section i to the elementary aerosol distribution $\phi^j(r)$ (9).

$$H_{ij} = \int \left[e \sum_q q G(i, z(q, r)) P(q, r) \right] \phi^j(r) dr. \quad (9)$$

2.5.1 Evaluation of the spectrum

The distribution is found by solving the apparatus equation (8) in respect to spectrum ϕ . The inversion is performed with the generalized least squares method (10).

$$\phi = \left(H^T D^{-1} H \right)^{-1} H^T D^{-1} y. \quad (10)$$

The measurement uncertainties are described by a covariance matrix D with the elements $D_{ii} = \Delta I_i^2$ being the individual variances of section currents. The uncertainty of the spectrum is then given by equation 11.

$$W = \left(H^T D^{-1} H \right)^{-1} \quad (11)$$

2.5.2 Regularization of the inversion

The information matrix (12) may be ill-posed – it may be impossible to invert it directly.

$$V = H^T D^{-1} H \quad (12)$$

The problem is avoided by using Tikhonov regularization (Tikhonov, 1963). The method allows to increase the rank of the matrix and thus to correct the ill-posedness (Lemmetty et al., 2005). The diagonal elements of V are amplified:

$$V'_{ij} = \begin{cases} V_{ij} & \text{if } i \neq j, \\ V_{ij} \cdot (1 + \lambda_i) & \text{if } i = j. \end{cases} \quad (13)$$

where λ is an arbitrary regularization vector.

A quasi-optimal regularization is reached by performing a two-pass inversion. Initially, to make the inversion possible at all, the regularization parameter is set to a small constant: $\lambda_i = 0.001$.

The second inversion is performed using a regularization vector based on uncertainty levels obtained from the first pass. The regularization vector λ is calculated as the ratio of error $W' = V'^{-1}$ to spectrum ϕ :

$$\lambda'_i = K \cdot \frac{W'_{ii}}{\phi_i^2} \quad (14)$$

where K is a constant in the range 0.1 to 1. The values of λ and K are not critical and are chosen during the calibration of an instrument.

2.5.3 Correction of negative concentration values

The inversion does not impose any constraints on the spectrum ϕ and so negative values can appear in the solutions for measurements at low concentrations. A simple procedure can be used to remove these.

If negative values appear, the inversion is repeated with the assumption that the previously most negative element of ϕ is virtually zero and the corresponding column in the instrument matrix is dropped. Usually two or three iterations are sufficient to remove all negative elements.

The procedure may increase the total concentration estimate. However, due to the nature of the inversion and significant overlapping of the elementary distributions, any correction of a spectrum element is balanced by changes in neighboring elements and the estimated spectrum still fits the measured currents. As a result, the effect remains below the level of measurement uncertainties.

3 Design of the Nanometer aerosol and Air Ion Spectrometer

The principle of electrical aerosol spectrometry is used by the Nanometer aerosol and Air Ion Spectrometer (NAIS). The NAIS is a multichannel aerosol instrument capable of measuring the distribution of ions (charged particles and cluster ions) of both polarities in the electric mobility range from 3.2 to $0.0013 \text{ cm}^2\text{V}^{-1}\text{s}^{-1}$ and the distribution of aerosol particles in the size range from 2.0 to 40 nm.

The instrument has been specifically designed for monitoring of atmospheric nanometer aerosol. It can operate for long periods in a wide range of ambient conditions from polluted downtown to remote forest to measure the size distributions of naturally charged particles (ions) of both polarities as well as uncharged particles.

The first NAIS was developed as an enhanced Air Ion Spectrometer (AIS, Mirme et al., 2007) in the year 2005. The only difference between the instruments was the updated aerosol sample preconditioning unit, which enabled the NAIS to optionally measure uncharged particles. In 2007 the development of a second generation NAIS was started. The primary motivation was to enable the instrument to operate at varying altitudes on board an aircraft, but also to improve the reliability of regular measurements.

3.1 General principle

The NAIS consists of two multichannel electrical mobility analyzer columns operating in parallel. The columns differ by the polarity of the ions measured, but are otherwise identical (Figure 3). The aerosol is synchronously mobility-classified in the mobility analyzers and measured with an array of 21 electrometers per column.

Both columns have a software controlled sample preconditioning unit in front of the analyzers which contains unipolar corona chargers and electric filters. By changing the setup of the preconditioning, the instrument can detect either only ions or all particles including the uncharged fraction.

The two similar measurement columns with opposite polarities in parallel allow the NAIS to detect variations of natural electric charge balance in the atmosphere and possible effects of electric charge polarity on charging of nanometer size aerosol.

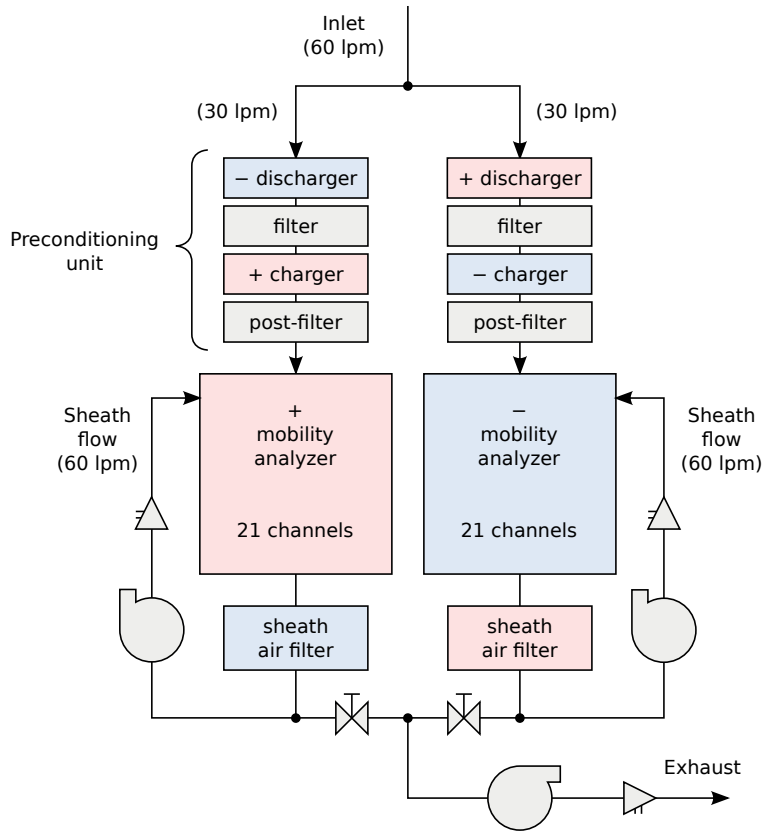


Figure 3: NAIS measurement flow process

3.2 Sample preconditioning

The sample preconditioning unit of the NAIS consists of a discharger, an electric filter, a charger and another electric filter (called the post-filter). The state of the chargers and filters determines what is detected by the mobility analyzer.

In *ions mode* all components of the preconditioning unit are switched off, so the aerosol sample is left unmodified and only naturally charged particles are sensed by the electric mobility analyzer. In this case the NAIS operates just like the AIS.

In *particles mode* the main charger is switched on and the instrument detects all particles. In this operating mode the NAIS is similar to the

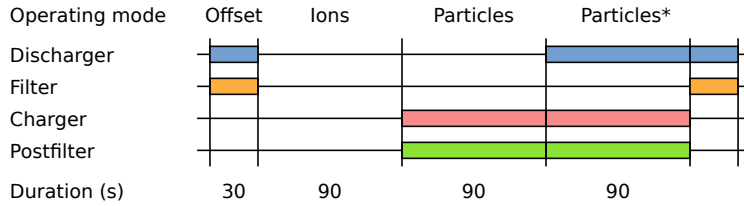


Figure 4: Typical measurement cycle of the NAIS. Offset measurements should be done for 20 – 30 seconds about every 5 minutes. Otherwise the user is free to choose the operating modes and their durations.

Electrical Aerosol Spectrometer (EAS, Tammet et al., 2002). The main charger is always used together with the post-filter which removes traces of charger ions.

To improve the instrument performance when measuring aerosol with non-steady state charge distribution, additionally the discharger may be switched on (*alternative charging mode*). This provides some neutralization of the aerosol sample and so reduces the effect of the particle initial charge on the measurement result.

When only the discharger and the adjacent filter are switched on, then no detectable particles can enter the analyzer. This is called the *offset mode* (zero mode). It is used to periodically verify the instrument operation (e.g. measure noise levels).

A typical measurement cycle is presented in figure 4.

3.2.1 Chargers

Each charger in the NAIS is essentially a corona needle on the axis of a cylindrical volume (Figure 5). The ions from the tip of the needle travel across the aerosol sample flow and attach to particles mainly by thermal diffusion. The charging ion concentration is maintained at a constant level by stabilizing the current that reaches the electrode surrounding the charging space.

The design of the discharger is similar to that of the subsequent main charger but it works in the opposite electrical polarity. In offset mode, when only the discharger is switched on, particles are charged to the wrong polarity for the respective analyzer, so the measured signal only consists of the parasitic (offset) currents and measurement noise. By knowing the offset sig-

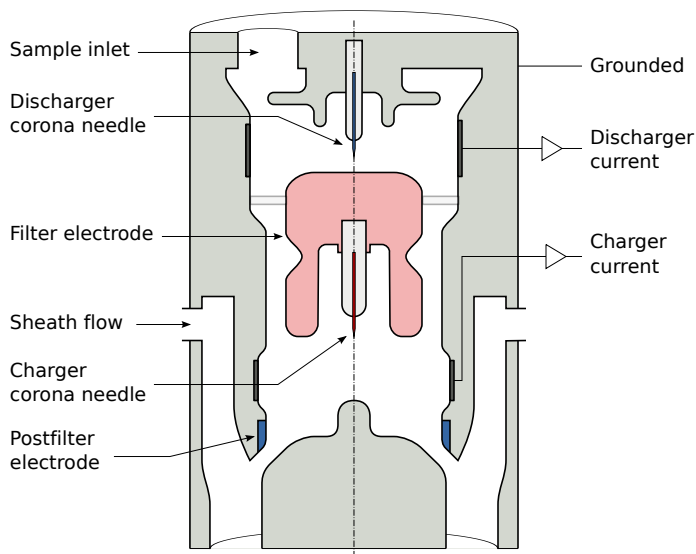


Figure 5: Schematic of NAIS charger

nal, measurement uncertainties can be significantly decreased and reliability of the results improved.

When the instrument operates in the particles measurement mode, the enabling of the discharger means that initially charged particles of either polarity are effectively discharged with opposite polarity charger ions in the discharger or main charger, depending on their initial charge.

It is important to keep the electric field strength in the charger volume as low as possible to minimize particle loss and simultaneously to keep the charger ion concentration as high as possible to maximize charging efficiency. So the charger is operated quite close to the corona ignition limit.

Corona discharge is inherently unstable. The NAIS uses a feedback system to adjust the voltage of the corona needle based on the electric current of charger ions to the outer electrode.

The upgraded NAIS employs a digital PID controller to adjust the charger voltage. The charger current target is specified in software. It may be different for the different operating modes of the instrument.

It is possible to use a pulsating corona voltage so that the average corona needle voltage is actually below the point of the corona ignition. Experiments of adding a periodic component to the corona voltage were carried out but

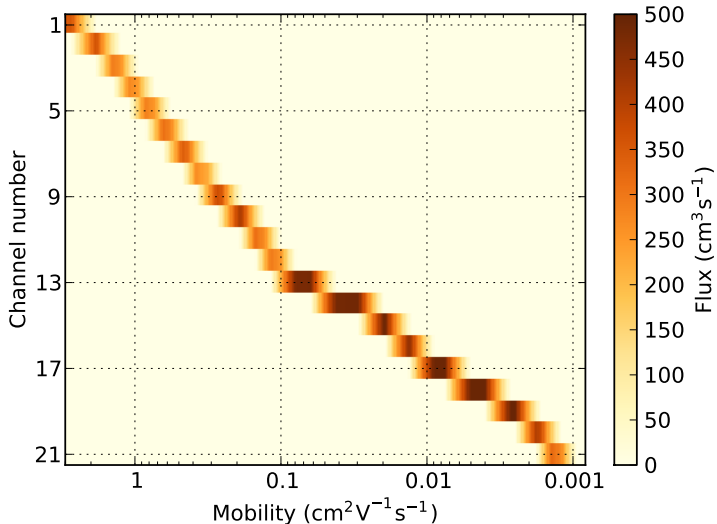


Figure 6: Analyzer response $G(i, z)$ for the NAIS. It can be seen that the responses for individual channels are overlapping. The total flux for any single mobility is $500 \text{ cm}^3 \text{ s}^{-1}$.

didn't yield much success and the idea was not used for the final instrument (Eller, 2009). The corona high-voltage power source generates a small high frequency (tens of kHz) ripple in its output. This proved to be sufficient and additional voltage modulation was unnecessary.

3.3 Mobility analysis

The mobility analysis in NAIS corresponds exactly to the parallel electrical aerosol measurement principle. The capacitances between the collecting sections and sections of central electrodes for the NAIS are presented in Table 1. The table also shows the voltages of the respective sections. Note that the collecting sections are not matched with the central sections: collecting sections 9, 13 and 17 have some capacitance with two adjacent central sections. This is used to cover a wide mobility range quite smoothly with a limited number of central sections. The calculated theoretical responses (transfer functions) for each section of the mobility analyzer are quite broad (Figure 6) and have a varying mobility resolution.

Table 1: The electrical capacitance (in pF) between collecting sections and the four central sections of the NAIS mobility analyzer. See Figure 6 for corresponding particle mobility ranges.

Collecting section	Central section (U_A)			
	9V	25V	220V	800V
0	3.030	0	0	0
1	2.531	0	0	0
2	2.433	0	0	0
3	2.504	0	0	0
4	2.913	0	0	0
5	3.860	0	0	0
6	5.597	0	0	0
7	8.250	0	0	0
8	8.716	0	0	0
9	4.006	4.526	0	0
10	0	8.693	0	0
11	0	8.741	0	0
12	0	9.850	0	0
13	0	5.850	5.235	0
14	0	0	10.656	0
15	0	0	11.149	0
16	0	0	13.558	0
17	0	0	11.784	8.061
18	0	0	0	19.053
19	0	0	0	25.330
20	0	0	0	25.472
21	0	0	0	25.510

3.3.1 Post-filter adjustment

The charger ions are in the same size range as the smallest particles measured by the instrument and so they would seriously disturb the first measurement channels of the mobility analyzer. The post-filter is used to remove these. The choice of the post-filter voltage is a compromise between charger ion penetration and removal of small particles.

The mobility of the corona ions depends on air temperature, relative humidity and the concentration of different gaseous impurities in air.

In the first generation NAIS instruments, the post-filter voltage could only be adjusted by hand and so a sensible value had to be set based on the experience of the instrument operator.

In the second generation instruments, the post-filter voltage can be adjusted by software and an algorithm has been developed that does it automatically. The principal idea is to keep the average current measured by the first channels of the analyzers at a constant low value. The algorithm has proven to be suitable for long term atmospheric monitoring. For laboratory experiments with rapidly changing or unusual aerosol distributions, it is better to switch the automatic adjustment off.

3.3.2 Airflows

Under NTP conditions the NAIS uses the sheath flow value $\Phi_s = 1000 \frac{\text{cm}^3}{\text{s}}$ and the sample flow value $\Phi_a = 500 \frac{\text{cm}^3}{\text{s}}$ (on newer instruments $450 \frac{\text{cm}^3}{\text{s}}$).

The upgraded NAIS automatically adjusts its sample and sheath airflow speeds so that the particle sizing and volume sample flow remain constant regardless of air pressure.

If we consider equation 2, the size of the classified particle remains invariant of air pressure if Φ_s and Φ_a are chosen so that the expression $\frac{\Phi_s + \Phi_a}{z}$ remains invariant of air pressure.

In case of small particles, for which the mean free path is much larger than particle radius, equation 4 can be simplified (Tammet, 1995). After substituting l and η , we get the equation 15:

$$\lim_{r \rightarrow 0} z_{\text{Millikan}} = \frac{e(a+b)}{6\pi r^2} \frac{1.256}{P} \sqrt{\frac{kT}{m_g}} \propto \frac{\sqrt{T}}{P} \quad (15)$$

where m_g is the mass of air molecule, P is air pressure and T is temperature.

In NAIS the sample flow rate Φ_a is kept constant. Considering equations 2 and 15 this means that the size classification remains air pressure invariant if Φ_s is chosen so that the following relation holds:

$$(\Phi'_s + \Phi'_a) \frac{\sqrt{T'}}{P'} = (\Phi_s + \Phi_a) \frac{\sqrt{T}}{P}, \quad (16)$$

where Φ'_s , Φ'_a , T' and P' are the corresponding variables under standard conditions. This allows the instrument to be used in varying conditions e.g. for airborne measurements (Mirme et al., 2010).

3.4 Electric current measurement

The electric currents collected on the outer electrodes are very small – in the range of 1 – 3 fA per electrode in the cluster ion range and even smaller in intermediate ion range (Hörrak, 2001).

The NAIS uses integrating electrometric amplifiers where the fluxes of electric charge are collected on high quality electrical capacitors. The output voltages of the amplifiers are proportional to the collected electric charge and the change of the voltage is proportional to incoming charge i.e to the aerosol current.

The integrating measurement principle allows for the best possible signal to noise ratio for electric current measurements. It is also well suited for the NAIS as the signal is collected continuously almost without any breaks – no signal is missed regardless of measurement frequency.

The voltage values from the amplifier outputs are read by an 24 bit analog-digital converter. The AIS instruments and older NAIS instruments used a quite slow converter which allowed to capture all the 42 voltages in about 10 seconds. This is sufficient for atmospheric monitoring where the signals are usually reduced to 2 – 5 minute averages.

For the updated NAIS a new data acquisition system was designed that can measure all electrometers 10 to 15 times per second. This allows us to use several additional signal processing steps to improve the results before averaging the signals and producing spectra (Figure 7). When measuring high concentrations even 1 – 10 second average spectra have sufficiently low signal-to-noise ratio to be useful.

3.4.1 Offset correction

Firstly the electric current values are corrected for the offset currents measured periodically during the offset operating mode. Also the estimated noise levels are bundled with the records and all further steps will always consider and operate on the signal and noise together. The offset correction and noise

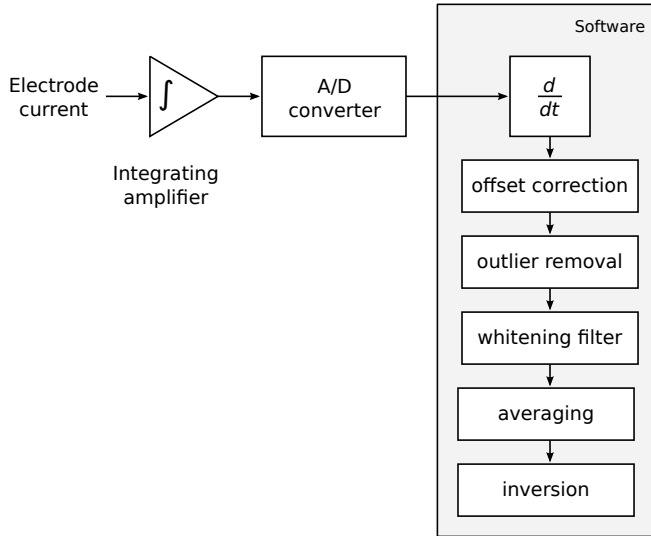


Figure 7: Signal-processing flow diagram of the NAIS.

estimates are essential to the data processing and have always been used with the AIS and NAIS instruments.

The offset signal is estimated using linear regression on the current measurements from previous and next offset measurement cycles (see Figure 4). This means that the final measurement result will be available after the next offset measurement cycle has been completed. The noise estimates are calculated from the difference between the regression estimate and actual offset signals.

3.4.2 Outlier removal

Often short spikes occur in the electric current signal that can't be the result of actual measured aerosol. Most likely their cause is the random decay of radioactive particles deposited on the electrodes. The frequency of spikes increases as more dirt is collected on the electrodes.

On older NAIS instruments it was not possible to detect these spikes because, due to the low measurement rate, the spikes were indistinguishable from proper signal. On the updated NAIS, a simple outlier detection algorithm is used to discard the false signal measurements. As long as the instrument is not too dirty, the spikes can be detected reliably.

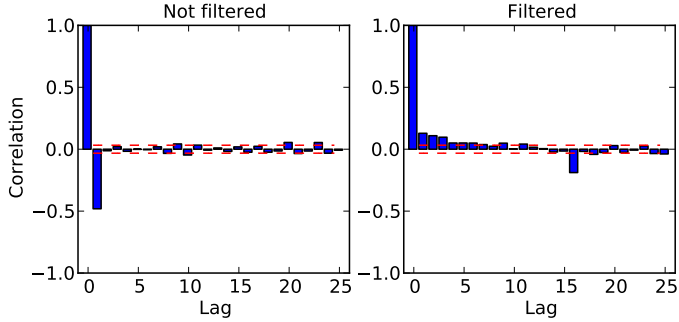


Figure 8: Autocorrelation function of electrometer signals without and with filtering. Here exponentially declining window function was used. It was truncated to 15 elements.

Table 2: Signal noise levels for raw and filtered signals at different averaging periods.

Averaging	none	1 s	10 s
Unfiltered signal noise (fA)	1.95	0.71	0.23
Filtered signal noise (fA)	0.85	0.46	0.15

3.4.3 Filtering

The excessively high measurement rate allows to employ optimal signal processing (ARMA filter). The electric current signal is passed through a matched digital filter to whiten the noise distribution. This improves the effectiveness of averaging in case of short periods, i.e. 1 to 10 seconds (Eller, 2008).

Autocorrelation analysis of the raw electrometer current signal shows a significant negative correlation between adjacent measurements. A filter was found that eliminates this (Figure 8) and consequently lowers signal noise levels in case of short averaging periods (Table 2). The filter decreases the time resolution by less than 0.5 seconds.

3.4.4 Electrometer resets

The collected charge on the capacitors needs to be cleared every once in a while. In NAIS the electrometers will automatically reset when the output signal reaches the upper or lower limit of the integrator. Signal from that electrometer is ignored for the duration of the reset and the settling,

which takes about ten seconds. At low concentrations resets can happen about once a day for each electrometer, which practically does not affect the measurements.

Thanks to the higher measurement rate, the moment of the electrometer reset is detected more precisely and no correct measurement signal has to be discarded.

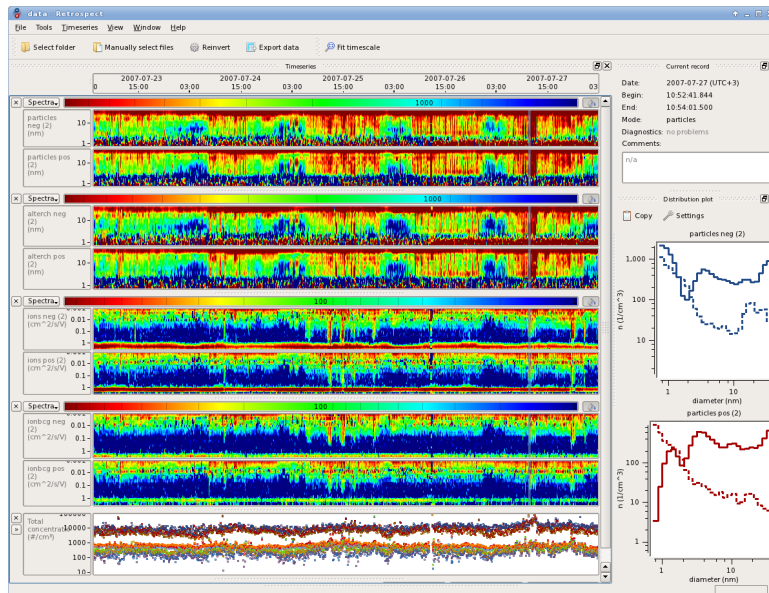


Figure 9: A screenshot of the developed NAIS data analysis software. In addition to particles, alternative charging, ions modes, the instrument has measured in ions-background mode, which is similar to ions mode but uses a added electric filter in the inlet tube. Similar plots are shown in real time during the measurements as well.

4 Results

There are more than ten NAIS instruments in use today around the world. The technology has been developed gradually and implemented into new instruments along the way. The first five instruments built were very similar to the AIS. New generation instruments have been built since 2008.

Typical measurement result of the instrument are presented in Figure 9.

4.1 Measurement campaigns

The instruments have been measuring in many places. For example:

- forest sites (in Finland: Kulmala et al., 2007b; in Australia: Suni et al., 2008)
- high altitudes (Venzac et al., 2007)
- the South-African savannah (Laakso et al., 2008; Vakkari et al., 2011)

- a marine environment in Ireland (Vana et al., 2008, Lehtipalo et al., 2010)
- Antarctica (Virkkula et al., 2007; Asmi et al., 2010)
- train trip from Moscow to Vladivostok (Vartiainen et al., 2007),
- indoors (Hirsikko et al., 2007)
- chamber experiment at CERN (CLOUD, Duplissy et al., 2010)
- on ships (Vana et al., 2007)
- on board an hot-air balloon (Laakso et al., 2007)
- on board an airplane (EUCAARI LONGREX, Mirme et al., 2010; Kulmala et al., 2010)

See also (Hirsikko et al., 2011; Manninen et al., 2009).

Between spring 2008 and spring 2009, the instruments were measuring at different EUCAARI stations (European Integrated Project on 25 Aerosol Cloud Climate Air Quality Interactions; Kulmala et al., 2009; Manninen et al., 2010; Kerminen et al., 2010)

4.2 Airborne measurements

The NAIS participated in the EUCAARI LONGREX measurement campaign in 2009 (Kulmala et al., 2009). The instrument flew on board the DLR Falcon research aircraft (Figure 10 and 11) in total about 50 flight hours (Figure 12). The measurements were successful (Mirme et al., 2010).

As altitude increased, air pressure decreased and particle mobilities increased, so the sheath flow pumps had to work exceedingly hard to hold the measurement size range constant. The air-flows were successfully controlled up to the 8-km altitude. Above that the sheath flow pumps were unable to provide the required flow rate. This caused the measurement range of the instrument to shift towards larger particles. It was possible to correct the size shift in post-processing of the data, but data about the smallest particles was lost as it was not measured.

Particle charging did not work ideally at higher altitudes. The decrease of air pressure caused the corona charger currents to increase and become less stable. At the 12-km altitude the average currents were about 130 % of their specified values, which caused some overcharging and may have resulted in an overestimation of particle concentrations by about 10–20 %. The elevated



Figure 10: DLR Falcon 20 high altitude research aircraft (photo courtesy of DLR)



Figure 11: The NAIS (the box instrument in light grey inside the rack) with connection to the sample air inlet on the top inside the Falcon aircraft.

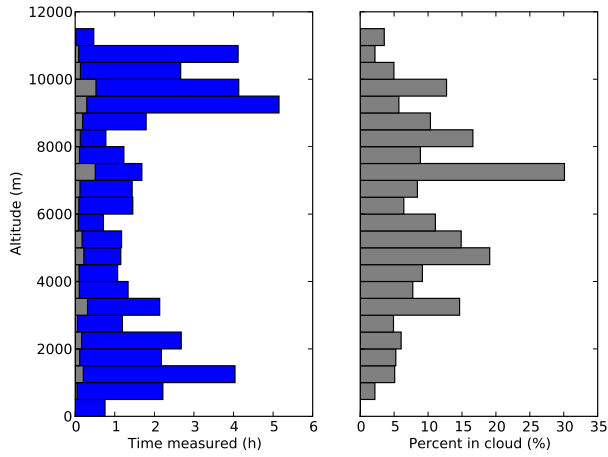


Figure 12: Amount of time the aircraft spent at different altitudes in total (blue bars) and in clouds (gray bars).

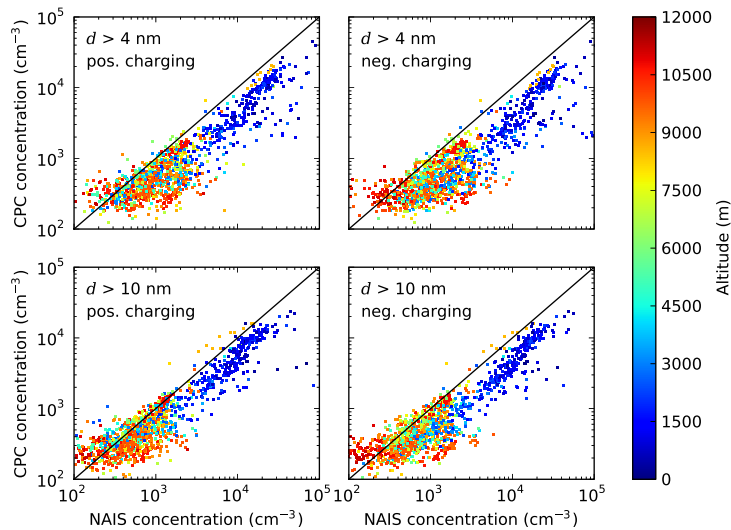


Figure 13: Comparison of concentrations measured using NAIS and CPC at different size ranges. The NAIS may have overestimated the concentrations due to overcharging. The CPC may have underestimated concentrations due to higher inlet losses.

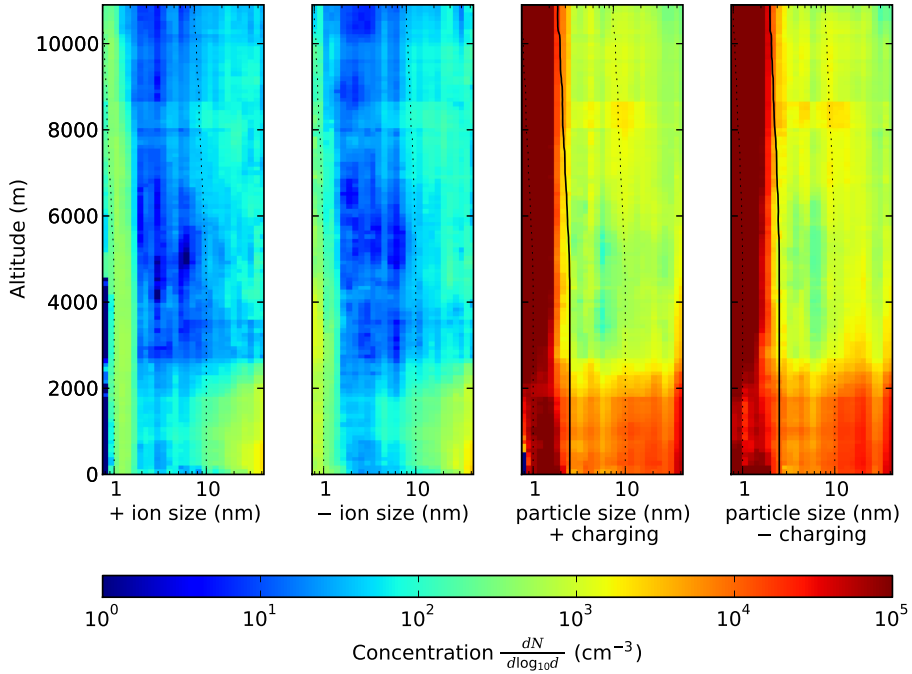


Figure 14: Median concentrations of positively and negatively charged clusters and particles (two panels on the left) measured using the NAIS at different altitudes from all the flights. Panels on the right display the corresponding total (neutral + charged) cluster / particle concentrations, as recorded by the two (positive and negative) polarity channels of the NAIS. Ions produced by the NAIS corona charger perturb the measurement of the smallest clusters on the two panels on the right. A detailed analysis shows that this perturbation affects only the size range <2 nm in the boundary layer, reaching the size of 2.5 nm at about the 7–8 km altitude. The limit of 2.5 nm has been marked with a solid black line in these panels.

charger currents led also to some leakage of charger ions through the post-filters and caused a high concentration of sub-2 nm particles to appear in the spectra. This limited the lower size of detectable particles at higher altitudes.

The NAIS was compared to two CPC-s on board the Falcon with cut-off sizes at 4 nm and 10 nm. The corresponding fraction concentrations calculated from the NAIS size distributions showed a good agreement between the instruments. The Pearson correlation coefficients range between 0.75 and 0.91 when considering results from all altitudes. Scatter-plots comparing the results from the CPC and the NAIS are presented in Fig. 13.

The NAIS was shown to measure reliably the concentrations and size distributions of neutral and charged particles down to mobility diameters of 2 – 2.5 nm throughout the tropospheric column (Figure 14).

4.3 Instrument verification

The calibration and verification of the NAIS is a complex task. All the instruments have been briefly tested and calibrated at the facilities of University of Tartu (Mirme et al., 2007). Their performance has been more thoroughly studied in several calibration and intercomparison experiments at the University of Helsinki.

In 2008, five NAIS and five AIS instruments were compared and calibrated at the University of Helsinki using high resolution and HAUKE type DMA-s for mobility references and a CPC and a aerosol electrometer for concentration references (Asmi et al., 2009). The NAIS-s overestimated the size of negative ions by 20 – 52% and the size of positive ions by 24 – 54%. The concentration measurements from NAIS were shown to be reliable at medium and high concentrations, at lower concentrations the NAIS-s showed some background noise.

In 2010, six NAIS and five AIS instruments were evaluated at the University of Helsinki regarding particle size/mobility and concentration using mobility standards and silver particles covering the size range between 1 and 40 nm (Gagné et al., 2011). The instruments were compared to a differential mobility particle sizer (DMPS), a BSMA (Tammet, 2006) and an Ion-DMPS. The experiments showed that the mobility detection of the AIS and NAIS instruments is reliable, provided that the instrument is clean and the flows are not obstructed. The NAIS can overestimate the concentration by a factor of 2 – 3 in the particles measurement mode.

5 Review of papers and author's contributions

Paper I (“Atmospheric sub-3 nm particles at high altitudes”) The paper reports the results of first and most important measurements of the new “Airborne”-NAIS instrument. These were the first ever airborne measurements of sub-3nm neutral particles at altitudes above the planetary boundary layer. I was the key person in developing the new generation NAIS and was responsible for performing the NAIS measurement during the airborne measurement campaign. I performed all the data processing and analysis, provided virtually all the figures for the paper and wrote 30% of the text.

Paper II (“EUCAARI ion spectrometer measurements at 12 European sites – analysis of new particle formation events”) The paper reports the results of a year-long measurement campaign from 12 European measurements sites. 11 NAIS and AIS instruments measured in many different environments. This confirmed the reliability of the technological solutions used by the instruments and showed their suitability for long term atmospheric monitoring. All the measurement and initial data processing software for the NAIS and AIS instruments was developed by me. I provided technical support and consulting to the various the measurement stations that used the instruments. I helped with the data processing and writing of the paper.

Paper III (“A wide range multi-channel Air Ion Spectrometer”) The paper describes the principles of the AIS, the predecessor of the NAIS instrument. I helped to develop the measurement and data analysis software and conducted mathematical modeling on the instrument. I helped to write the paper.

6 Conclusions

The main conclusions of the thesis are:

The NAIS has proven to be capable of measuring alternately nanometer aerosol and cluster-ions.

The NAIS instruments have been successfully used for long term atmospheric monitoring and they have detected nucleation events everywhere around the world where they have measured.

A new generation NAIS has been developed that is capable of correctly measuring in low pressure environments.

The NAIS has been successfully used to measure sub-3 nm aerosol particles from on board an aircraft throughout the tropospheric column.

References

- Asmi, E., Frey, A., Virkkula, A., Ehn, M., Manninen, H. E., Timonen, H., Tolonen-Kivimäki, O., Aurela, M., Hillamo, R., & Kulmala, M. (2010). Hygroscopicity and chemical composition of antarctic sub-micrometre aerosol particles and observations of new particle formation. *Atmos. Chem. Phys.*, 10(9), 4253–4271.
- Asmi, E., Sipilä, M., Manninen, H. E., Vanhanen, J., Lehtipalo, K., Gagné, S., Neitola, K., Mirme, A., Mirme, S., Tamm, E., Uin, J., Komsaare, K., Attoui, M., & Kulmala, M. (2009). Results of the first air ion spectrometer calibration and intercomparison workshop. *Atmos. Chem. Phys.*, 9(1), 141–154.
- Boisdrón, T. & Brock, J. R. (1970). On the stochastic nature of the acquisition of electric charge and radioactivity by aerosol particles. *Atmos. Environ.*, 4, 35–50.
- Duplissy, J., Enghoff, M. B., Aplin, K. L., Arnold, F., Aufmhoff, H., Avn-gaard, M., Baltensperger, U., Bondo, T., Bingham, R., Carslaw, K., Curtius, J., David, A., Fastrup, B., Gagné, S., Hahn, F., Harrison, R. G., Kellett, B., Kirkby, J., Kulmala, M., Laakso, L., Laaksonen, A., Lillestol, E., Lockwood, M., Mäkelä, J., Makhmutov, V., Marsh, N. D., Nieminen, T., Onnela, A., Pedersen, E., Pedersen, J. O. P., Polny, J., Reichl, U., Seinfeld, J. H., Sipilä, M., Stozhkov, Y., Stratmann, F., Svensmark, H., Svensmark, J., Veenhof, R., Verheggen, B., Viisanen, Y., Wagner, P. E., Wehrle, G., Weingartner, E., Wex, H., Wilhelmsson, M., & Winkler, P. M. (2010). Results from the CERN pilot CLOUD experiment. *Atmos. Chem. Phys.*, 10(4), 1635–1647.
- Eller, M. (2008). Signal processing in aerosol fast measurements. Master's thesis, University of Tartu, Estonia.
- Eller, M. (2009). Stabilizing the measurements with electrical aerosol spectrometer EAS. Master's thesis, University of Tartu, Estonia.
- Fuchs, N. A. (1963). *Geofis. Pura Appl.*, 56.
- Fuchs, N. A. (1964). The mechanics of aerosols.
- Gagné, S., Lehtipalo, K., Manninen, H. E., Nieminen, T., Schobesberger, S., Franchin, A., Yli-Juuti, T., Boulon, J., Sonntag, A., Mirme, S., Mirme, A., Hörrak, U., Petäjä, T., Asmi, E., & Kulmala, M. (2011). Intercomparison

- of air ion spectrometers: an evaluation of results in varying conditions. *Atmospheric Measurement Techniques*, 4(5), 805–822.
- Hirsikko, A., Nieminen, T., Gagné, S., Lehtipalo, K., Manninen, H. E., Ehn, M., Hörrak, U., Kerminen, V.-M., Laakso, L., McMurry, P. H., Mirme, A., Mirme, S., Petäjä, T., Tammet, H., Vakkari, V., Vana, M., & Kulmala, M. (2011). Atmospheric ions and nucleation: a review of observations. *Atmos. Chem. Phys.*, 11(2), 767–798.
- Hirsikko, A., Yli-Juuti, T., Nieminen, T., Vartiainen, E., Laakso, L., Hussein, T., & Kulmala, M. (2007). Indoor and outdoor air ions and aerosol particles in the urban atmosphere of helsinki: characteristics, sources and formation. *Boreal Environment Research*, 12(3), 295–310.
- Hörrak, U. (2001). *Air ion mobility spectrum at a rural area*. PhD thesis, University of Tartu.
- Israel, H. (1931). Zur theorie und methodik der grossenbestimmung von luftionen. *Gerlands Beitr. Geophys*, 31, 173–216.
- Jakobson, A., Salm, J., & Tammet, H. (1975). Some results of testing the multichannel automatic spectrometer of air ions. *In acta et commentationes Universitatis Tartuensis*, 348, 16–23.
- Kerminen, V.-M., Petäjä, T., Manninen, H. E., Paasonen, P., Nieminen, T., Sipilä, M., Junninen, H., Ehn, M., Gagné, S., Laakso, L., Riipinen, I., Vehkamäki, H., Kurten, T., Ortega, I. K., Dal Maso, M., Brus, D., Hyvärinen, A., Lihavainen, H., Leppä, J., Lehtinen, K. E. J., Mirme, A., Mirme, S., Hörrak, U., Berndt, T., Stratmann, F., Birmili, W., Wiedensohler, A., Metzger, A., Dommen, J., Baltensperger, U., Kiendler-Scharr, A., Mentel, T. F., Wildt, J., Winkler, P. M., Wagner, P. E., Petzold, A., Minikin, A., Plass-Dülmer, C., Pöschl, U., Laaksonen, A., & Kulmala, M. (2010). Atmospheric nucleation: highlights of the EUCAARI project and future directions. *Atmos. Chem. Phys.*, 10(22), 10829–10848.
- Kulmala, M., Asmi, A., Lappalainen, H. K., Carslaw, K. S., Pöschl, U., Baltensperger, U., Hov, Ø., Brenquier, J.-L., Pandis, S. N., Facchini, M. C., Hansson, H.-C., Wiedensohler, A., & O’Dowd, C. D. (2009). Introduction: European integrated project on aerosol cloud climate and air quality interactions (EUCAARI) – integrating aerosol research from nano to global scales. *Atmos. Chem. Phys.*, 9(8), 2825–2841.

- Kulmala, M., Mordas, G., Petäjä, T., Grönholm, T., Aalto, P., Vehkamäki, H., Gaman, A., Herrmann, E., Sipilä, M., Riipinen, I., Manninen, H., Hämeri, K., Stratmann, F., Birmili, W., & Wagner, P. E. (2007a). The condensation particle counter battery (CPCB): A new tool to investigate the activation properties of nanoparticles. *J. Aerosol Sci.*, 38, 289 – 304.
- Kulmala, M., Riipinen, I., Nieminen, T., Hulkkonen, M., Sogacheva, L., Manninen, H. E., Paasonen, P., Petäjä, T., Dal Maso, M., Aalto, P. P., Viljanen, A., Usoskin, I., Vainio, R., Mirme, S., Mirme, A., Minikin, A., Petzold, A., Hörrak, U., Plaß-Dülmer, C., Birmili, W., & Kerminen, V.-M. (2010). Atmospheric data over a solar cycle: no connection between galactic cosmic rays and new particle formation. *Atmos. Chem. Phys.*, 10(4), 1885–1898.
- Kulmala, M., Riipinen, I., Sipilä, M., Manninen, H. E., Petäjä, T., Junninen, H., Maso, M. D., Mordas, G., Mirme, A., Vana, M., Hirsikko, A., Laakso, L., Harrison, R. M., Hanson, I., Leung, C., Lehtinen, K. E., & Kerminen, V.-M. (2007b). Towards direct measurement of atmospheric nucleation. *Science*, 318(5847), 89–92.
- Kulmala, M., Vehkimäki, H., Petäjä, T., Maso, M., Lauri, A., Kerminen, V.-M., Birmili, W., & McMurry, P. H. (2004). Formation and growth rates of ultrafine atmospheric particles: A review of observations. *J. Aerosol Sci.*, 35, 143–176.
- Laakso, L., Groenholm, T., Kulmala, L., Haapanala, S., Hirsikko, A., Lovejoy, E., Kazil, J., Kurten, T., Boy, M., Nilsson, E., et al. (2007). Hot-air balloon as a platform for boundary layer profile measurements during particle formation. *Boreal Environment Research*, 12(3), 279–294.
- Laakso, L., Laakso, H., Aalto, P. P., Keronen, P., Petäjä, T., Nieminen, T., Pohja, T., Siivola, E., Kulmala, M., Kgabi, N., Molefe, M., Mabaso, D., Phalatse, D., Pienaar, K., & Kerminen, V.-M. (2008). Basic characteristics of atmospheric particles, trace gases and meteorology in a relatively clean southern african savannah environment. *Atmos. Chem. Phys.*, 8(16), 4823–4839.
- Lehtipalo, K., Kulmala, M., Sipilä, M., Petäjä, T., Vana, M., Ceburnis, D., Dupuy, R., & O’Dowd, C. (2010). Nanoparticles in boreal forest and coastal environment: a comparison of observations and implications of the nucleation mechanism. *Atmos. Chem. Phys.*, 10(15), 7009–7016.

- Lemmetty, M., Marjamäki, M., & Keskinen, J. (2005). The ELPI response and data reduction II: Properties of kernel and data inversion. *Aerosol Sci. Technol.*, 39, 583–595.
- Manninen, H., Petäjä, T., Asmi, E., Riipinen, I., Nieminen, T., Mikkilä, J., Horrak, U., Mirme, A., Mirme, S., Laakso, L., et al. (2009). Long-term field measurements of charged and neutral clusters using neutral cluster and air ion spectrometer (nais). *Boreal Env. Res*, 14, 591–605.
- Manninen, H. E., Nieminen, T., Asmi, E., Gagné, S., Häkkinen, S., Lehtipalo, K., Aalto, P., Vana, M., Mirme, A., Mirme, S., Hörrak, U., Plass-Dülmer, C., Stange, G., Kiss, G., Hoffer, A., Törö, N., Moerman, M., Henzing, B., de Leeuw, G., Brinkenberg, M., Kouvarakis, G. N., Bougiatioti, A., Mihalopoulos, N., O’Dowd, C., Ceburnis, D., Arneth, A., Svenningsson, B., Swietlicki, E., Tarozzi, L., Decesari, S., Facchini, M. C., Birmili, W., Sonntag, A., Wiedensohler, A., Boulon, J., Sellegri, K., Laj, P., Gysel, M., Bukowiecki, N., Weingartner, E., Wehrle, G., Laaksonen, A., Hamed, A., Joutsensaari, J., Petäjä, T., Kerminen, V.-M., & Kulmala, M. (2010). EUCAARI ion spectrometer measurements at 12 European sites – analysis of new particle formation events. *Atmos. Chem. Phys.*, 10(16), 7907–7927.
- Marti, J. J., Weber, R. J., Saros, M. T., Vasiliou, J. G., & McMurry, P. H. (1996). Modification of the TSI 3025 condensation particle counter for pulse height analysis. *Aerosol Sci. Technol.*, 25-2, 214 – 218.
- McMurry, P. (2000). The history of condensation nucleus counters. *Aerosol science and technology*, 33(4), 297–322.
- Mirme, A., Noppel, M., Peil, I., Salm, J., Tamm, E., & Tammet, H. (1984). Multi-channel electric aerosol spectrometer. In *Intern. Comm. for Cloud Phys. 11 th Intern. Conf. on Atmosphere Aerosols, Condensation and Ice Nuclei.*, volume 2 (pp. 155–159).
- Mirme, A., Tamm, E., Mordas, G., Vana, M., Uin, J., Mirme, S., Bernotas, T., Laakso, L., Hirsikko, A., & Kulmala, M. (2007). A wide range multi-channel air ion spectrometer. *Boreal Env. Res.*, 12, 247–264.
- Mirme, S., Mirme, A., Minikin, A., Petzold, A., Hörrak, U., Kerminen, V.-M., & Kulmala, M. (2010). Atmospheric sub-3 nm particles at high altitudes. *Atmos. Chem. Phys.*, 10(2), 437–451.

- Podolsky, A. (1977). On the computation of the time of capturing ions by aerosol particle. *In acta et commentationes Universitatis Tartuensis*, 443, 62–73.
- Salm, J. (1992). Unipolar charging of initially charged aerosol. *Acta et comm. Univ. Tartuensis*, 947, 68–71.
- Suni, T., Kulmala, M., Hirsikko, A., Bergman, T., Laakso, L., Aalto, P. P., Leuning, R., Cleugh, H., Zegelin, S., Hughes, D., van Gorsel, E., Kitchen, M., Vana, M., Hörrak, U., Mirme, S., Mirme, A., Sevanto, S., Twining, J., & Tardos, C. (2008). Formation and characteristics of ions and charged aerosol particles in a native Australian eucalypt forest. *Atmos. Chem. Phys.*, 8(1), 129–139.
- Tammet, H. (1970). *The aspiration method for the Determination of Atmospheric-Ion Spectra*. The Israel Program for Scientific Translations Jerusalem. Washington, D.C.: National Science Foundation.
- Tammet, H. (1992). On the techniques of aerosol electrical granulometry. *Acta et comm. Univ. Tartuensis*, 947, 94–115.
- Tammet, H. (1995). Size and mobility of nanometer particles, clusters and ions. *J. Aerosol Sci.*, 26(3), 459–475.
- Tammet, H. (2006). Continuous scanning of the mobility and size distribution of charged clusters and nanometer particles in atmospheric air and the Balanced Scanning Mobility Analyzer BSMA. *Atmospheric research*, 82(3-4), 523–535.
- Tammet, H. (2011). Symmetric inclined grid mobility analyzer for the measurement of charged clusters and fine nanoparticles in atmospheric air. *Aerosol Science and Technology*, 45(4), 468–479.
- Tammet, H., Mirme, A., & Tamm, E. (2002). Electrical aerosol spectrometer of Tartu University. *Atmos. Res.*, 62 (3-4), 315–324.
- Tikhonov, A. N. (1963). Solution of incorrectly formulated problem and the regularization method. *Soviet Math. Dokl.*, 4, 1035–1038.
- Vakkari, V., Laakso, H., Kulmala, M., Laaksonen, A., Mabaso, D., Molefe, M., Kgabi, N., & Laakso, L. (2011). New particle formation events in semi-clean South African savannah. *Atmos. Chem. Phys.*, 11(7), 3333–3346.

- Vana, M., Ehn, M., Petaja, T., Vuollekoski, H., Aalto, P., de Leeuw, G., Ceburnis, D., O'Dowd, C., & Kulmala, M. (2008). Characteristic features of air ions at mace head on the west coast of ireland. *Atmospheric Research*, 90(2-4), 278–286.
- Vana, M., Virkkula, A., Hirsikko, A., Aalto, P., Kulmala, M., & Hillamo, R. (2007). Air ion measurements during a cruise from Europe to Antarctica. In *Nucleation and Atmospheric Aerosols: 17th International Conference, Galway, Ireland, 2007* (pp. 368).: Springer Verlag.
- Vartiainen, E., Kulmala, M., Ehn, M., Hirsikko, A., Junninen, H., Petaejae, T., Sogacheva, L., Kuokka, S., Hillamo, R., Skorokhod, A., et al. (2007). Ion and particle number concentrations and size distributions along the trans-siberian railroad. *Boreal Env. Res.*, 12(3), 375–396.
- Venzac, H., Sellegri, K., & Laj, P. (2007). Nucleation events detected at the high latitude site of the puy de dome research station, france. *Boreal Env. Res.*, 12, 345–359.
- Virkkula, A., Hirsikko, A., Vana, M., Aalto, P., Hillamo, R., & Kulmala, M. (2007). Charged particle size distributions and analysis of particle formation events at the finnish antarctic research station aboa. *Boreal Environment Research*, 12(3), 397–408.
- Wang, S. & Flagan, R. (1990). Scanning electrical mobility spectrometer. *Aerosol Science and Technology*, 13(2), 230–240.
- Yunker, E. A. (1940). The mobility-spectrum of atmospheric ions. *Terrestrial magnetism and atmospheric electricity*, 45(2), 127–132.

Acknowledgements

The research for this thesis was carried out at the Institute of Physics, University of Tartu. Many resources were provided by Airel Ltd.

I thank my supervisor Dr. Aadu Mirme for his encouragement and support.

I'm very grateful to the researchers at the Division of Atmospheric Sciences at the University of Helsinki for their close cooperation. I wish to specially thank Prof. Markku Kulmala for his support of the development of aerosol instrumentation in Tartu.

I thank all the researchers who have used the NAIS instrument to gain interesting new knowledge about the world. I am specially grateful to all the people who have written papers about this research and taken me as a co-author.

I'd like to thank the German Aerospace Center, Institute for Atmospheric Physics for the opportunity to make the most exciting aerosol measurements with the NAIS instrument yet.

I thank my parents.

Financial support by Estonian Research Council (project SF0180043s08 and grants 8342, 8417) and European Commission 6th Framework programme project EUCAARI, contract no 036833-2 (EUCAARI) is gratefully acknowledged.

Summary in Estonian

Nanomeeter-aerosooli mõõtmistehnoloogia arendamine

Aerosooliosakeste teket nukleatsiooni teel ja nende järgnevat kasvu on jälgitud kõikjal maailmas. Tekkinud osakesed on algselt nanomeetri suurusel, kuid võimelised kasvama ja seejärel osalema pilvetekkes, muutma kiirgusbilanssi ja lõpuks mõjutama Maa kliimat. Samuti võivad nano-osakesed mõjuda inimeste tervisele.

Aerosooliosakeste tekke uurimise vastu on suur huvi, kuid nanomeetri-suuruste osakeste mõõtmine atmosfääris on keerukas.

Osakeste tekke uurimiseks sobib hästi nanomeeter-aerosooli ja õhuhioonide spektromeeter (NAIS, välja töötatud AS Airel, Eesti). Seade kasutab elektrilise aerosooli spektromeetria põhimõtet, et mõõta nii elektriliselt laetud osakeste (aero-ioonide) või ka laadimata osakeste suuruspektreid. Spektromeeter on suuteline töötama kaua hooldusvabalt väga erinevates keskkondades – nii reostunud kesklinnast, kui ka kaugetes metsades. Seade on väljatöötatud aeroioonide spektromeetri (AIS) baasil.

NAIS tööpõhimõte seisneb aerosooli laadimises unipolaarses korona ioonide väljas ja paralleelses elektrilises liikuvusanalüüsis. NAIS-il on kaks paljukanalist elektrilist liikuvusanalüsaatorit, üks positiivsete ja teine negatiivsete laengute detekteerimiseks. Aerosool klassifitseeritakse ja mõõdetakse mõlemas analüsaatoris samaaegselt, kummaski 21 elektromeetriga. Seade mõõdab ionide (laetud osakeste, klasterioonide) liikuvusjaotust vahemikus $3.2 - 0.0013 \text{ cm}^2 \text{ V}^{-1} \text{ s}^{-1}$ ja aerosooliosakeste suurusjaotust vahemikus 2.0 – 40 nm. Hetkel on üle maailma käigus üle kümne NAIS mõõteseadme.

Väitekiri põhineb NAIS spektromeeter arendusel. Kirjeldatakse seadme matemaatilisi ja tehnilisi põhimõtteid. Tutvustatakse uut edasiarendatud NAIS mudelit – nn. “Lendav NAIS”, mis on suuteline sooritama mõõtmisi lennukilt laias kõrgustevahemikus. Uue seadme parandatud töökindlus, paindlikkus ja mõõtmiskiirus tulevad kasuks ka tavapärasel “maistel” atmosfäärimõõtmistel.

Publications

Curriculum Vitae

Name: Sander Mirme

Birth: 13 February 1981, Tartu

Citizenship: Estonian

Address: Institute of Physics, Tähe 4, Tartu 51010, Estonia

Phone: (+327) 56650016

E-mail: sander.mirme@ut.ee

Education:

2005 – 2011 University of Tartu, PhD studies
2003 – 2005 University of Tartu, masters studies
1999 – 2003 University of Tartu, bachelor studies

Languages: Estonian (mother tongue), English, German

Carreer: 2007 - ... University of Tartu, engineer

Main research fields:

Aerosol spectrometry, measurement methods,
instrumentation development.

Curriculum Vitae in Estonian

Nimi: Sander Mirme

Sünd: 13 veebruar 1981, Tartu

Kodakondsus: Estonian

Aaddress: Füüsika instituut, Tähe 4, Tartu 51010, Estonia

Telefon: (+327) 56650016

E-mail: sander.mirme@ut.ee

Haridus:

2005 – 2011 Tartu Ülikool, PhD õpingud

2003 – 2005 Tartu Ülikool, magistrantuur

1999 – 2003 Tartu Ülikool, bakalaureuseõpe

Keeled: eesti (emakeel), inglise, saksa

Teenistuskäik: 2007 - ... University of Tartu, insener

Peamine uurimisvaldkond:

aerosooli spektrometria, mõõtmismeetodid,
mõõteaparatuuri arendus.

DISSERTATIONES GEOPHYSICALES UNIVERSITATIS TARTUENSIS

1. **Andres Kuusk.** The hot-spot effect in plant canopy reflectance. Tartu, 1991.
2. **Tiit Nilson.** Radiative transfer in non-homogeneous plant canopies. Tartu, 1991.
3. **Helgi Arst.** Atmosfääri ja mere kiirguskarakteristikud looduskeskkonna seisundi informaatoritena (vene keeles). Tartu, 1991.
4. **Juha Sarkkula.** Measuring and modelling water currents and quality as a part of decision making process for water pollution control. Tartu, 1992.
5. **Piia Post.** On the two radiatively effective cloud parameters. Tartu, 1993.
6. **Aadu Mirme.** Electric aerosol spectrometry. Tartu, 1994.
7. **Aare Luts.** Mathematical simulation of the evolutions of air ions. Tartu, 1995.
8. **Tiit Kutser.** Estimation of water quality in turbid inland and coastal waters by passive optical remote sensing. Tartu, 1997.
9. **Ülle Kikas.** Atmospheric aerosol in the Baltic region. Tartu, 1998.
10. **Tarmo Kõuts.** Processes of deep water renewal in the Baltic sea. Tartu, 1999.
11. **Anu Reinart.** Underwater light field characteristics in different types of Estonian and Finnish lakes. Tartu, 2000.
12. **Marko Kaasik.** Parameterisation of atmospheric boundary layer in the numerical model of air pollution transport. Tartu, 2000.
13. **Janek Laanearu.** Topographically constrained deep-water flows in channels. Tartu, 2001.
14. **Urmas Raudsepp.** Wind-driven circulation in the gulf of Riga. Tartu, 2001.
15. **Urmas Hõrrak.** Air ion mobility spectrum at a rural area. Tartu, 2001.
16. **Marko Vana.** Formation and evolution of atmospheric aerosol size spectrum by the occurrence of nucleation burst events in the atmospheric boundary layer; transport of the climatically active particulate air pollution. Tartu, 2002.
17. **Veljo Kimmel.** Analysis of methods of air quality assessment. Applications in Estonia. Tartu, 2002.
18. **Oleg Okulov.** Variability of atmospheric transparency and precipitable water in Estonia. Tartu, 2003.
19. **Aarne Männik.** Implementation and validation of the nonhydrostatic adiabatic core of the numerical weather prediction model hirlam. Tartu, 2003.
20. **Matti Mõttus.** Shortwave solar radiation field inside willow canopy. Tartu, 2004.
21. **Kalev Rannat.** Long weakly nonlinear waves in geophysical applications. Tartu, 2007.

22. **Rigel Kivi.** Observations of ozone, polar stratospheric cloud and water vapour profiles in the arctic. Tartu, 2007.
23. **Erko Jakobson.** Spatial and temporal variability of atmospheric column humidity. Tartu, 2009.